Plant Cell Physiol. 48(6): 886–891 (2007)
doi:10.1093/pcp/pcm054, available online at www.pcp.oxfordjournals.org

Short Communication

Enzymatic Activity and Motility of Recombinant *Arabidopsis* Myosin XI, MYA1

You Hachikubo [1], Kohji Ito [1], John Schiefelbein [2], Dietmar J. Manstein [3] and Keiichi Yamamoto [1,*]

[1] *Department of Biology, Chiba University, Inageku, Chiba, 263-8522 Japan*
[2] *Department of Molecular, Cellular, and Developmental Biology, University of Michigan, MI, USA*
[3] *Institute for Biophysical Chemistry, Hannover Medical School, Hannover, Germany*

We expressed recombinant *Arabidopsis* myosin XI (MYA1), in which the motor domain of MYA1 was connected to an artificial lever arm composed of triple helical repeats of *Dictyostelium* α-actinin, in order to understand its motor activity and intracellular function. The V_{max} and K_{actin} of the actin-activated Mg^{2+} ATPase activity of the recombinant MYA1 were 50.7 Pi head^{-1} s^{-1} and 30.2 μM, respectively, at 25°C. The recombinant MYA1 could translocate actin filament at the maximum velocity of 1.8 μm s^{-1} at 25°C in the in vitro motility assay. The value corresponded to a motility of 3.2 μm s^{-1} for native MYA1 if we consider the difference in the lever arm length, and this value was very close to the velocity of cytoplasmic streaming in *Arabidopsis* hypocotyl epidermal cells. The extent of inhibition by ADP of the motility of MYA1 was similar to that of the well-known processive motor, myosin V, suggesting that MYA1 is a processive motor. The dissociation rate of the actin–MYA1-ADP complex induced by ATP (73.5 s^{-1}) and the V_{max} value of the actin-activated Mg^{2+} ATPase activity revealed that MYA1 stays in the actin-bound state for about 70% of its mechanochemical cycle time. This high ratio of actin-bound states is also a characteristic of processive motors. Our results strongly suggest that MYA1 is a processive motor and involved in vesicle transport and/or cytoplasmic streaming.

Keywords: *Arabidopsis* — ATPase — Motility — MYA1 — Myosin — Processivity.

Abbreviations: BSA, bovine serum albumin; DTT, dithiothreitol; eYFP, enhanced yellow fluorescent protein; 2ME, 2-mercaptoethanol.

Myosin is a molecular motor that uses ATP as an energy source and moves along actin filaments. Phylogenetic analysis of all the myosins sequenced so far revealed that there are at least 24 classes of myosin (Foth et al. 2006), though only three myosin classes, VIII, XI and XIII, were found in plants (Knight and Kendrick-Jones 1993, Kinkema and Schiefelbein 1994, Vugrek et al. 2003). Myosins play important functional roles within plant cells in driving actin-based motility such as intracellular vesicle transport and cytoplasmic streaming (Reddy 2001). Although many plant myosin genes have been cloned, only a few have been purified and characterized biochemically because they are labile and susceptible to proteolytic degradation (Yokota and Shimmen 1994, Yamamoto et al. 1994, Ito et al. 2003, Tominaga et al. 2003, Wang and Pesacreta 2004)

There are 17 myosin genes in *Arabidopsis*, and four of them belong to class VIII myosin and 13 to class XI (Reddy and Day 2001). Holweg and Nick (2004) showed that knockout of a class XI myosin (MYA2) of *Arabidopsis* by T-DNA insertion caused severe inhibition in growth, fertility and auxin transport. On the other hand, Hashimoto et al. (2005) reported that growth and fertility of *Arabidopsis* did not change by deletion of the MYA2 gene. These authors also reported that an antibody raised against a peptide with a sequence specific for MYA2 co-localized with peroxisomes, suggesting the association of MYA2 with this organelle, but cells of mutant *Arabidopsis* in which MYA2 was deleted did not show any change in the distribution of peroxisomes. In general, knockout of one myosin gene in plants does not show prominent changes in phenotype, suggesting functional overlap among these gene products

To understand the specific function of these myosins in plant cells, characterization of their motor activity is indispensable. The motor activity of myosin may be characterized by the ATPase activity, the motility and the processivity. The processivity is the ability of myosin to move on a single actin filament for a long distance without detaching from it, and is a very important characteristic for a myosin participating in intracellular vesicle transport. This processive movement can be achieved only when each head of two-headed myosin stays on an actin filament for >50% of its mechanochemical cycle time. In this study,

*Corresponding author: E-mail, yamamoto@bio.s.chiba-u.ac.jp; Fax, +81-43-290-2809.

we connected the motor domain of *Arabidopsis* myosin MYA1 (class XI) to an artificial lever arm consisting of triple helical repeats 1 and 2 of *Dictyostelium* α-actinin (Anson et al. 1996), expressed it in *Dictyostelium* cells and characterized its motor activity. The triple helical repeats 1 and 2 of *Dictyostelium* α-actinin are a rod-like part of the molecule with a length of about 12 nm (Kliche et al. 2001) and do not have actin-binding sites. We have to use this artificial lever arm because essential components of the natural MYA1 lever arm, light chains, are not well understood. Expressing myosin in a recombinant form with the artificial lever arm was used at first to show that the motility of myosin is proportional to the lever arm length (Anson et al. 1996). The recombinant technique was also successfully used to show that cloned *Chara* myosin cDNA is exactly that of a myosin responsible for the very fast cytoplasmic streaming (Ito et al. 2003).

We made two recombinant constructs, MYA1-2R-Y and MYA1-2R, in this study (Fig. 1a). MYA1-2R-Y is composed of the motor domain of MYA1 (1–736) followed by a rigid domain consisting of triple helical repeats 1 and 2 of *Dictyostelium* α-actinin, a flexible linker (GSGGSGGSGGS), enhanced yellow fluorescent protein (eYFP) and a $(His)_8$-tag. MYA1-2R has a myc-tag instead of eYFP. These constructs are similar in structure to the skeletal muscle myosin subfragment-1. The expression vectors for the production of MYA1-2R-Y and MYA1-2R were generated as described in Materials and Methods. The constructs were overproduced in myosin II null mutant cells of *Dictyostelium* (HS1) and purified as described in Materials and Methods. The observed molecular weights of MYA1-2R-Y and MYA1-2R were 145 and 115 kDa, respectively (Fig. 1b). These values were identical to those predicted from their amino acid sequences. Yield and purity of both MYA1-2R-Y and MYA1-2R were about 0.2 mg per 10 g wet cells and >85%, respectively (Fig. 1b). MYA1-2R-Y was used for the in vitro motility assay because commercially available anti-green fluorescent protein (GFP) antibody could effectively tether the YFP portion of the construct (distal end of the lever arm) to the glass surface. MYA1-2R was used for the kinetic study, because the YFP portion of MYA1-2R-Y might interfere with the optical measurements used in a stopped flow apparatus.

The basal ATPase activity of MYA1-2R in the absence of actin was 0.029 Pi head^{-1} s^{-1} at 25°C. The ATPase activity of MYA1-2R showed hyperbolic dependence on actin concentration (Fig. 2a), and the V_{max} and K_{actin} (the concentration of actin that enhances the ATPase activity to a half of the V_{max}) were obtained by fitting the curve to the Michaelis–Menten equation. The V_{max} and K_{actin} of MYA1-2R were 50.7 Pi head^{-1} s^{-1} and 30.2 μM, respectively.

To investigate the motility of MYA1-2R-Y, we used an antibody-based version of the in vitro actin filament gliding assay in which the construct was fixed to a glass surface by anti-GFP monoclonal antibody (Ito et al. 2003). The movement of fluorescent actin filaments was recorded on videotape and analyzed as described previously (Awata et al. 2001). As mentioned in Materials and Methods, we treated assay chambers with unlabeled F-actin and ATP to block the disturbance of actin filament translocation by denatured MYA1-2R-Y. MYA1-2R-Y supported smooth continuous movement of actin filaments, indicating that the unlabeled F-actin effectively blocked denatured MYA1-2R-Y. MYA1-2R-Y translocated actin filaments at the maximum velocity of 1.8 μm s^{-1} and the average

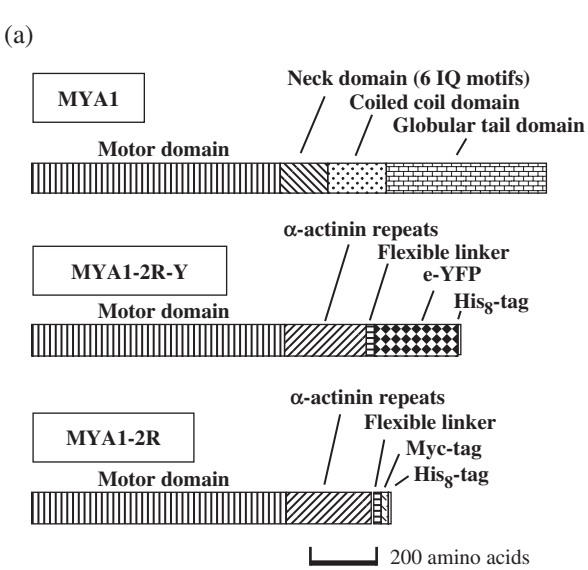

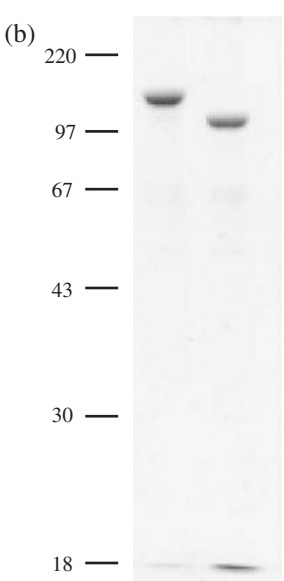

Fig. 1 (a) Schematic diagrams showing the sequence features of MYA1-2R-Y and MYA1-2R, together with MYA1. (b) SDS–polyacrylamide gel electrophoresis of purified MYA1-2R-Y (left) and MYA1-2R (right). The acrylamide concentration was 12%. The positions of the molecular weight markers are indicated on the left (kDa).

velocity of $0.98 \pm 0.33\ \mu m\ s^{-1}$ at 25°C (Fig. 2b). The number of actin filaments measured was 183.

The mechanochemical cycle of myosin (M) and actin (A) with bound nucleotides can be summarized as follows.

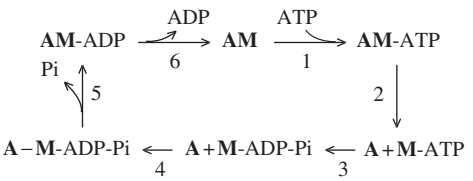

Myosin and actin bind tightly in the absence of ATP but they dissociate when ATP enters the active site of myosin and causes a structural change in myosin (steps 1 and 2). Myosin hydrolyzes ATP (step 3) and interacts with actin weakly at first (step 4). This interaction becomes strong, and myosin generates a mechanical force when inorganic phosphate is released (step 5). Then ADP is released and myosin and actin return to the initial state (step 6). To move on a single actin filament without detaching from it (processive movement), one head of two-headed myosin must rebind to actin before the other head dissociates from actin. This processive movement can be achieved only when each head of myosin stays in an actin-bound state (upper row in the scheme) for >50% of its mechanochemical cycle time. Most of the known processive myosins stay in the actin-bound state for a long time due to their high affinity for ADP and slow ADP release from the actin–myosin-ADP complex (Wang et al. 2000; step 6). The motility of processive motors such as myosin V is generally inhibited by ADP more severely than that of non-processive motors such as skeletal muscle myosin II because processive motors have higher affinity for ADP and it competes for the active site with ATP.

To investigate whether MYA1 is a processive motor or not, we first examined the effect of ADP on the motility of MYA1-2R-Y at a constant ATP concentration (2 mM). The sliding velocity of actin filaments decreased with the increase in the ADP concentration. At an ADP concentration of 2 mM (molar ratio to ATP is 1 : 1), the sliding velocity of actin filaments decreased to 25% of that attained in the absence of ADP (Fig. 3). This profile was similar to that of the processive motor, myosin V (Wang et al. 2000; broken line in Fig. 3). The effect of ADP on the motility of skeletal muscle myosin (non-processive motor; Homsher et al. 1993) is also shown by the dotted line in Fig. 3.

As mentioned above, each head of the processive myosins stays in the actin-bound state (upper row in the scheme) for >50% of its mechanochemical cycle time due to slow ADP release from the actin–myosin-ADP complex (Wang et al. 2000; step 6 in the scheme). The mechanochemical cycle time of MYA1-2R can be calculated from

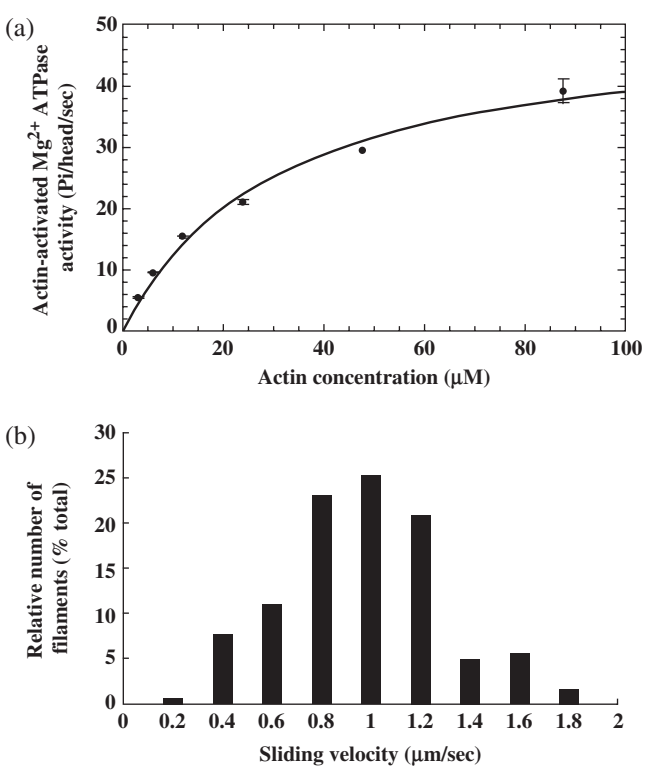

Fig. 2 (a) The actin-activated ATPase activity of MYA1-2R. (b) Histogram showing the distribution of sliding velocity of actin filaments over the MYA1-2R-Y-coated surface in the in vitro motility assay.

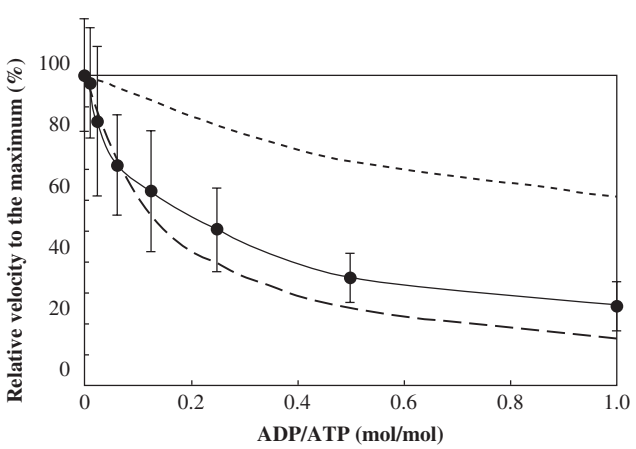

Fig. 3 The effect of ADP on the sliding velocity of actin filaments on a MYA1-2R-Y-coated surface (filled circles). The ADP concentration was varied from 0 to 2 mM while the ATP concentration was held at 2 mM. The experiment was done at 25°C. Each data point is an average of 30–60 filaments in three independent experiments, and bars indicate the standard deviation. For comparison, the effects of ADP on the sliding velocity of actin filaments on a myosin V-coated surface (typical processive motor, broken line) (Wang et al. 2000) and on a skeletal muscle myosin II-coated surface (typical non-processive motor, dotted line) (Homsher et al. 1993) are shown.

the V_{max} value of actin-activated ATPase activity. The value is 50.7 Pi head^{-1} s^{-1} (Fig. 2a) and the cycle time is 19.7 ms. To estimate the time of actin-bound states in the mechanochemical cycle of MYA1-2R, we measured the rate of ATP-induced dissociation of the actin–MYA1-2R-ADP complex using the stopped flow technique. This process includes ADP release from actin–MYA1-2R (step 6), entry of ATP to the active site of MYA1-2R (step 1) and dissociation of MYA1-2R-ATP from actin (step 2). The ADP release rate, the ATP binding rate and the dissociation rate of MYA1-2R-ATP from actin define the time spent in the actin–MYA1-2R-ADP state, actin–MYA1-2R state and actin–MYA1-2R-ATP state, respectively (upper row in the scheme). The time course of ATP-induced dissociation of the actin–MYA1-2R-ADP complex observed by the decrease in the light scattering is shown in Fig. 4. The data fitted well with a single exponential curve and gave a k_{obs} value of 73.5 s^{-1}. The total time spent in the actin-bound states is, therefore, 13.6 ms. Thus MYA1-2R stays on actin for about 70% of the duration of its mechanochemical cycle.

In this study, we tried to characterize the motor activity of *Arabidopsis* myosin XI, MYA1, using recombinant constructs. Recombinant MYA1 translocated actin filaments at a maximum velocity of 1.8 μm s^{-1} at 25°C. According to the lever arm theory, actin sliding velocity is proportional to the length of the lever arm (Anson et al. 1996, Uyeda et al. 1996). The length of the lever arm is the sum of the length of converter region and neck domain. The converter region is a part of the motor domain and changes its structure during the mechanochemical cycle of myosin and rotates around a fulcrum. The length from the fulcrum to the distal end of the converter is estimated to be 3 nm (Ito et al. 2003). The neck domain corresponds to the light chain-binding sites in the case of MYA1, or to α-actinin repeats in the case of MYA1-2R-Y (Fig. 1a). The length of one light chain-binding site is 4 nm as judged from the crystal structure of skeletal muscle myosin subfragment-1 (Rayment et al. 1993), and MYA1 has six light chain-binding sites (Kinkema and Schiefelbein 1993). The length of the α-actinin repeats is 12 nm (Kliche et al. 2001). Thus the estimated lever arm length of native MYA1 and MYA1-2R-Y is 27 and 15 nm, respectively. The maximum velocity of native MYA1 calculated from that of MYA1-2R-Y (1.8 μm s^{-1}) according to the lever arm theory is, therefore, 3.2 μm s^{-1}.

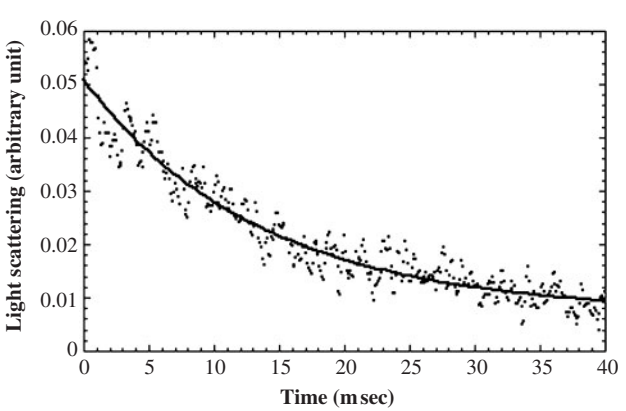

Fig. 4 ATP-induced dissociation of the actin–MYA1-2R-ADP complex. The decrease in the light scattering intensity was followed after rapidly mixing the actin–MYA1-2R-ADP complex with excess ATP. The experiment was done at 25°C. The smooth line represents the fitted single exponential curve. The rate constant k_{obs} was 73.5 s^{-1}.

If MYA1 is a processive motor, it moves along the actin filament in a hand-over-hand manner and the sliding velocity can be calculated as follows:

$$\text{sliding velocity} = \text{ATPase activity of two heads}\left(\text{Pi}\,\text{s}^{-1}\right) \times \text{step size}.$$

If we assume that the ATPase activity per head is the same as that of recombinant MYA1 and that the step size is the same as that of tobacco myosin, which belongs to the same class XI and has the same number of light chain-binding sites (IQ motifs) at the neck, the ATPase activity of the two heads is 101 Pi s^{-1} (Fig. 2a) and the step size is 35 nm (Tominaga et al. 2003). The velocity calculated by this formula was 3.5 μm s^{-1}. The two calculated values of sliding velocity were in good agreement with the cytoplasmic streaming velocity (2.5–3 μm s^{-1}) of *Arabidopsis* hypocotyl epidermal cells (Holweg and Nick 2004). Reisen and Hanson (2007) recently expressed a fusion protein of the MYA1 tail domain and YFP in various plant cells and showed that the protein co-localized with unidentified vesicles that move at a velocity of about 1 μm s^{-1}. If these vesicles were those transported by MYA1, the velocity of MYA1 in the cell is about 1 μm s^{-1}. However, YFP fusion proteins containing other *Arabidopsis* myosin XIs also co-localized with similar vesicles and moved at similar velocities, suggesting that these vesicles were not specifically driven by MYA1.

Our results suggested that MYA1 had other characteristics of a processive motor. The motility of MYA1-2R-Y was inhibited severely by ADP (Fig. 3). This indicates that the affinity of ADP for MYA1-2R-Y is quite strong and it competes for the active site with ATP. MYA1-2R stays in the actin-bound states for about 70% of its mechanochemical cycle time (Fig. 4). This characteristic will allow two-headed native MYA1 to move on a single actin filament for a long distance without detaching from it and to participate in organelle transport and/or cytoplasmic streaming.

The enzymatic activity and the motility of other plant class XI myosins have already been measured. Well documented myosins are 175 kDa myosin from tobacco BY-2 (Yokota et al. 1999, Tominaga et al. 2003) and that

from *Chara corallina* (Yamamoto et al. 1994, Awata et al. 2001, Ito et al. 2003). The former moves processively at a velocity of 9 μm s^{-1} with the maximum ATPase activity of 77 Pi $head^{-1}$ s^{-1}, and the latter moves non-processively at a velocity of 50 μm s^{-1} with the maximum ATPase activity of 400 Pi $head^{-1}$ s^{-1}. Because the number of plant myosins documented so far was very small, the structural features that make class XI myosins move processively or not and make them move at different average velocities are not well understood at present. It could be clarified by increasing the number of myosins characterized at the protein level.

We showed, in this study, that the recombinant motor domain with an artificial lever arm is useful to characterize plant myosins whose motor properties are not known. As there is no need for co-expression of any myosin light chains, this expression system can also be used to characterize myosins from other sources. The advantage of using a YFP fusion of a motor protein is that it can be used to estimate both enzymatic activity and motility. We can test the processivity of a myosin by examining the effect of ADP on its motility (Fig. 3). Such information will allow us to speculate on the intracellular function of various kinds of myosins that are recognized only by their sequences.

Materials and Methods

The expression vectors for the production of MYA1-2R-Y and MYA1-2R were generated as follows. Plasmid pBlue script MYA1 contained the full-length sequence of MYA1 (Kinkema and Schiefelbein, 1994) and had a *Bam*HI site in front of the ATG start codon. An *Xho*I site was created following Ala736 of the MYA1 sequence by site-directed mutagenesis using the ExSite PCR-Based Site-Directed Mutagenesis Kit (Stratagene, La Jolla, CA, USA). The sequences of the oligonucleotides used to create the mutations were 5′-TTACAAAGCTTGTATAAAGCCGAAC AATGTTC-3′ and 5′-TTGACTAGTTGCTCGAGAGGCAGCA TTCCCAAG-3′. The resultant plasmid, pBlue script MYA1 motor domain, encoded Met1–Ala736 of the MYA1 heavy chain. This plasmid was cut with *Xho*I and *Sac*I, and ligated with an *Xho*I–*Sac*I fragment from pM790-2R-eYFP (S. Zimmermann and D. J. Manstein, unpublished work) which has Gln266–Asp503 of *Dictyostelium* α-actinin, a flexible linker (GSGGSGGSGGSG), eYFP and a $(His)_8$-tag. The resultant plasmid encodes MYA1 heavy chain residues 1–736 followed by Gln266–Asp503 of *Dictyostelium* α-actinin, a flexible linker (GSGGSGGSGGSG), eYFP and a $(His)_8$-tag. This plasmid was cut with *Bam*HI and *Sac*I, and ligated with a *Bam*HI–*Sac*I fragment from pTIKL MyDAp that is a *Dictyostelium* myosin II expression vector (Liu et al. 2000). The resultant plasmid pTIKL MYA1-2R-Y encodes MYA1 heavy chain residues 1–736 followed by *Dictyostelium* α-actinin, the flexible linker, eYFP and a $(His)_8$-tag. The expression vector for the production of MYA1-2R was generated as follows. Plasmid pTIKL MYA1-2R-Y was cut with *Xho*I and *Sac*I, and ligated with an *Xho*I–*Sac*I fragment from pGEM72 actinin-myc-his (K. Ito and K. Yamamoto, unpublished work) which has a α-actinin, a flexible linker (GSGGSGGSGGSG), myc-tag and a $(His)_8$-tag. The resultant plasmid pTIKL MYA1-2R encodes MYA1 heavy chain residues 1–736 followed by *Dictyostelium* α-actinin, the flexible linker, myc-tag and a $(His)_8$-tag. pTIKL MYA1-2R-Y and pTIKL MYA1-2R were electroporated into *Dictyostelium* HS1 cells, a myosin II null strain, and transformants were selected in the presence of 18 μg ml^{-1} G418 in the HL-5 medium containing 6 μg ml^{-1} each of penicillin and streptomycin.

MYA1-2R and MYA1-2R-Y were purified according to the procedure of Manstein and Hunt (1995) with slight modification. All procedures were carried out at 0–4°C. Transformed HS1 cells at a density of 4×10^6–7×10^6 cells ml^{-1} were harvested by centrifugation at 1,100×*g* for 7 min. The pelleted cells were washed with 25 vol g^{-1} cells of a solution containing 0.04% NaN_3 and 10 mM Tris–HCl (pH 7.4), and then resuspended in 3 vol g^{-1} cells of a lysis buffer containing 50 mM KCl, 2.5 mM EDTA, 0.1 mM EGTA, 5 mM dithiothreitol (DTT), 25 mM HEPES (pH 8.0), 0.04% NaN_3 and a mixture of proteinase inhibitors (100 μM *p*-toluenesulfonyl-L-lysine chloromethyl ketone, 200 μM phenylmethylsulfonyl fluoride, 200 μM 1,10-phenanthroline, 20 μM leupeptin, 6 μM pepstatin and 200 μM *N*-*p*-tosyl-L-arginine methyl ester). The suspension was mixed with 3 vol g^{-1} cells of the lysis buffer supplemented with 0.6% Triton X-100, incubated on ice for 1 h, and then centrifuged at 38,000×*g* for 1 h. The pellet was suspended in 6 vol g^{-1} cells of a wash buffer containing 150 mM KCl, 2 mM EDTA, 1 mM DTT, 30 mM HEPES (pH 8.0) and a mixture of proteinase inhibitors, and the suspension was centrifuged at 38,000×*g* for 1 h. The washed pellet was extracted with 1.5 vol g^{-1} cells with an extraction buffer containing 100 mM KCl, 10 mM $MgCl_2$, 8 mM ATP, 7 mM 2-mercaptoethanol (2ME) and 30 mM HEPES (pH 7.0), and then the solution was centrifuged at 250,000×*g* for 1 h. The supernatant was loaded onto a column containing 200 μl of Ni-nitrilotriacetic acid agarose resin (Qiagen, Hilden, Germany). The column was washed extensively with a solution containing 5 mM imidazole, 300 mM KCl, 4 mM $MgCl_2$, 1 mM ATP, 10 mM 2ME and 25 mM HEPES (pH 7.4), followed by a second extensive wash with a solution containing 10 mM imidazole, 300 mM KCl, 4 mM $MgCl_2$, 1 mM ATP, 10 mM 2ME and 25 mM HEPES (pH 7.4). MYA1-2R and MYA1-2R-Y were eluted with 1 ml of 250 mM imidazole and 10 mM 2ME, and dialyzed against a buffer containing 25 mM KCl, 4 mM $MgCl_2$, 2 mM DTT and 25 mM HEPES (pH 7.4). Rabbit skeletal muscle actin was prepared according to the method of Spudich and Watt (1971).

An antibody-based version of the in vitro sliding filament assay was done according to the method of Reck-Peterson et al. (2001) with modification. Briefly, a flow chamber (9 × 3 mm, chamber volume about 4 μl) was prepared using a nitrocellulose-coated coverslip and a slide glass, as described by Kron et al. (1991). First, protein G (0.5 mg ml^{-1} in HEPES, pH 7.4, Zymed Laboratories, San Francisco, CA, USA) was allowed to bind to the glass surface of the assay chamber for 30 min at room temperature. The chamber was washed four times with 100 μl of a solution containing 150 mM NaCl and 10 mM HEPES, pH 7.4 (HBS). Next, anti-GFP monoclonal antibody (0.4 mg ml^{-1} in HBS, Sigma, St Louis MO, USA; Cat. No. G6539) was introduced into the chamber and left for 6–12 h at 4°C. After the antibody adsorption, the chamber was washed four times with 100 μl of HBS. Then, MYA1-2R-Y (0.1–0.2 mg ml^{-1} in HBS) was introduced into the chamber and left for 1–3 h at 4°C. The MYA1-2R-Y preparation generally contains a small amount of denatured protein. Such denatured MYA1-2R-Y cannot translocate actin filaments but, because it can still bind to it, disturbs the smooth movement of actin filaments. Before the introduction of F-actin labeled with rhodamine–phalloidin, the myosin-coated assay chamber was

washed with unlabeled F-actin and Mg^{2+}ATP in order to block residual denatured MYA1-2R-Y. The assay buffer used in the in vitro motility assay contained 25 mM KCl, 4 mM $MgCl_2$, 1 mM EGTA, 2 mM ATP, 20 mM DTT, 25 mM HEPES (pH 7.4), 12.8 mM glucose, 120 μg ml^{-1} glucose oxidase and 20 μg ml^{-1} catalase. The in vitro motility assay was performed at 25°C. Average sliding velocity was determined by measuring the displacement of actin filaments that moved smoothly for a distance >10 μm.

Steady-state ATPase activity was determined by measuring released phosphate using the method of Kodama et al. (1986) with modification. We added 1 mg ml^{-1} bovine serum albumin (BSA) to the reaction mixture to prevent adsorption of MYA1-2R to the surface of plastic tubes and to stabilize the enzyme. The reaction mixture for the assay of the basal Mg^{2+}ATPase activity contained 25 mM KCl, 4 mM $MgCl_2$, 1 mM DTT, 2 mM ATP, 25 mM HEPES (pH 7.4), 1 mg ml^{-1} BSA and 3 μg ml^{-1} MYA1-2R. The reaction mixture for the assay of actin-activated Mg^{2+}ATPase activity contained 25 mM KCl, 4 mM $MgCl_2$, 1 mM DTT, 2 mM ATP, 25 mM HEPES (pH 7.4), 1 mg ml^{-1} BSA, 3–95 μM F-actin and 3.5–30 nM MYA1-2R. We arranged the concentration of MYA1-2R so as to keep the concentration of ADP generated by the hydrolysis of ATP during the reaction lower than 0.1 mM because ADP may suppress the activity of MYA1-2R. The purity of the ATP used was satisfactorily high as judged from the ion exchange chromatogram, and contamination of ADP was negligible. The reactions were initiated by the addition of ATP and F-actin at 25°C. The reaction time for the basal Mg^{2+}-ATPase activity was 20–60 min and that for the actin-activated Mg^{2+}-ATPase activity was 5 min.

Stopped-flow measurement was performed using an Applied Photophysics SX18MV stopped-flow spectrophotometer. ATP-induced dissociation of the actin–MYA1-2R-ADP complex was measured by monitoring the decrease in the light scattering at 310 nm. The concentrations of MYA1-2R, F-actin and ADP in one syringe were 150 nM, 500 nM and 40 μM, respectively. The concentration of ATP in the other syringe was 8 mM. Assays were carried out at 25°C in a buffer containing 25 mM KCl, 4 mM $MgCl_2$, 1 mM DTT and 25 mM HEPES (pH 7.4). Data were analyzed by the least squares fitting procedure (Kaleidagraph, Abelbeck Software).

References

Anson, M., Geeves, M.A., Kurzawa, S.E. and Manstein, D.J. (1996) Myosin motors with artificial lever arms. *EMBO J.* 15: 6069–6074.

Awata, J., Saitoh, K., Shimada, K., Kashiyama, T. and Yamamoto, K. (2001) Effect of Ca^{2+} and calmodulin on the motile activity of Characean myosin in vitro. *Plant Cell Physiol.* 42: 828–834.

Foth, B.J., Goedecke, M.C. and Soldati, D. (2006) New insights into myosin evolution and classification. *Proc. Natl Acad. Sci. USA* 103: 3681–3686.

Hashimoto, K., Igarashi, H., Nishimura, M., Shimmen, T. and Yokota, E. (2005) Peroxisomal localization of a myosin XI isoform in *Arabidopsis thaliana*. *Plant Cell Physiol.* 46: 782–789.

Holweg, C. and Nick, P. (2004) Arabidopsis myosin XI mutant is defective in organelle movement and polar auxin transport. *Proc. Natl Acad. Sci. USA* 101: 10488–10493.

Homsher, E., Wang, F. and Sellers, J. (1993) Factors affecting filament velocity in in vitro motility assays and their relation to unloaded shortening velocity in muscle fibers. *Adv. Exp. Med. Biol.* 332: 279–290.

Ito, K., Kashiyama, T., Shimada, K., Yamaguchi, A., Awata, J., Hachikubo, Y., Manstein, D.J. and Yamamoto, K. (2003) Recombinant motor domain constructs of *Chara corallina* myosin display fast motility and high ATPase activity. *Biochem. Biophys. Res. Commun.* 312: 958–964.

Kinkema, M. and Schiefelbein, J. (1994) A myosin from a higher plant has structural similarities to class V myosins. *J. Mol. Biol.* 239: 591–597.

Kliche, W., Fujita-Becker, S., Kollmar, M., Manstein, D.J. and Kull, F.J. (2001) Structure of a genetically engineered molecular motor. *EMBO J.* 20: 40–46.

Knight, A.E. and Kendrick-Jones, J. (1993) A myosin-like protein from a higher plant. *J. Mol. Biol.* 231: 148–154.

Kodama, T., Fukui, K. and Kometani, K. (1986) The initial phosphate burst in ATP hydrolysis by myosin and subfragment-1 as studied by a modified malachite green method for determination of inorganic phosphate. *J. Biochem.* 99: 1465–1472.

Kron, S.J., Toyoshima, Y.Y., Uyeda, T.Q. and Spudich, J.A. (1991) Assays for actin sliding movement over myosin-coated surfaces. *Methods Enzymol.* 196: 399–416.

Liu, X., Ito, K., Lee, R.J. and Uyeda, T.Q. (2000) Involvement of tail domains in regulation of *Dictyostelium* myosin II. *Biochem. Biophys. Res. Commun.* 271: 75–81.

Manstein, D.J. and Hunt, D.M. (1995) Over expression of myosin motor domains in Dictyostelium: screening of transformants and purification of the affinity tagged protein. *J. Muscle Res. Cell Motil.* 16: 325–332.

Rayment, I., Rypniewski, W.R., Schmidt-Base, K., Smith, R., Tomchick, D.R., Benning, M.M., Winkelmann, D.A., Wesenberg, G. and Holden, H.M. (1993) Three-dimensional structure of myosin subfragment-1: a molecular motor. *Science* 261: 50–58.

Reck-Peterson, SL., Tyska, M.J., Novick, P.J. and Mooseker, M.S. (2001) The yeast class V myosins, Myo2p and Myo4p, are nonprocessive actin-based motors. *J. Cell Biol.* 153: 1121–1126.

Reddy, A.S.N. (2001) Molecular motors and their functions in plants. *Int. Rev. Cytol.* 204: 97–178.

Reddy, A.S.N. and Day, I.S. (2001) Analysis of the myosins encoded in the recently completed *Arabidopsis thaliana* genome sequence. *Genome Biol.* 2: 1–17.

Reisen, D. and Hanson, M.R. (2007) Association of six YFP–myosin XI-tail fusions with mobile plant cell organelles. *BMC Plant Biol.* 7: 6.

Spudich, J.A. and Watt, S. (1971) The regulation of rabbit skeletal muscle contraction. I. Biochemical studies of the interaction of the tropomyosin–troponin complex with actin and the proteolytic fragments of myosin. *J. Biol. Chem.* 246: 4866–4871.

Tominaga, M., Kojima, H., Yokota, E., Orii, H., Nakamori, R., Katayama, E., Anson, M., Shimmen, T. and Oiwa, K. (2003) Higher plant myosin XI moves processively on actin with 35 nm steps at high velocity. *EMBO J.* 22: 1263–1272.

Uyeda, T.Q., Abramson, P.D. and Spudich, J.A. (1996) The neck region of the myosin motor domain acts as a lever arm to generate movement. *Proc. Natl Acad. Sci. USA* 93: 4459–4464.

Vugrek, O., Sawitzky, H. and Menzel, D. (2003) Class XIII myosins from the green alga Acetabularia: driving force in organelle transport and tip growth? *J. Muscle Res. Cell Motil.* 24: 87–97.

Wang, F., Chen, L., Arcucci, O., Harvey, E.V., Bowers, B., Xu, Y., Hammer, J.A. and Sellers, J.R. (2000) Effect of ADP and ionic strength on the kinetic and motile properties of recombinant mouse myosin V. *J. Biol. Chem.* 275: 4329–4335.

Wang, Z. and Pesacrete, T.C. (2004) A subclass of myosin XI is associated with mitochondria, plastids and the molecular chaperone subunit TCP-alpha in maize. *Cell Motil. Cytoskel.* 57: 218–232.

Yamamoto, K., Kikuyama, M., Sutoh-Yamamoto, N. and Kamitsubo, E. (1994) Purification of actin-based motor protein from *Chara corallina*. *Proc. Jpn. Acad.* 70: 175–180.

Yokota, E. and Shimmen, T. (1994) Isolation and characterization of plant myosin from pollen tubes of lily. *Protoplasma* 177: 153–162.

Yokota, E., Yukawa, C., Muto, S., Sonobe, S. and Shimmen, T. (1999) Biochemical and immunocytochemical characterization of two types of myosins in cultured tobacco bright yellow-2 cells. *Plant Physiol.* 121: 525–534.

(Received March 27, 2007; Accepted May 6, 2007)